Received: 16 March 2022 | Revised: 12 December 2022 | Accepted: 9 January 2023

DOI: 10.1002/hbm.26212

RESEARCH ARTICLE

WILEY

In vivo characterization of magnetic resonance imaging-based T1w/T2w ratios reveals myelin-related changes in temporal lobe epilepsy

Yuchao Jiang[1,2] | Wei Li[3] | Yingjie Qin[3] | Le Zhang[3] | Xin Tong[3] | Fenglai Xiao[3] | Sisi Jiang[1,2] | Yunfang Li[4] | Qiyong Gong[5] | Dong Zhou[3] | Dongmei An[3] | Dezhong Yao[1,6,7] | Cheng Luo[1,2,6]

[1]The Clinical Hospital of Chengdu Brain Science Institute, MOE Key Lab for Neuroinformation, Center for Information in Medicine, University of Electronic Science and Technology of China, Chengdu, People's Republic of China

[2]High-Field Magnetic Resonance Brain Imaging Key Laboratory of Sichuan Province, School of life Science and technology, University of Electronic Science and Technology of China, Chengdu, People's Republic of China

[3]Department of Neurology, West China Hospital, Sichuan University, Chengdu, People's Republic of China

[4]Southern Medical District, Chinese People's Liberation Army General Hospital, Beijing, People's Republic of China

[5]Huaxi MR Research Center, Department of Radiology, West China Hospital, Sichuan University, Chengdu, People's Republic of China

[6]Research Unit of NeuroInformation, Chinese Academy of Medical Sciences, Chengdu, People's Republic of China

[7]Department of Neurology, First Affiliated Hospital of Hainan Medical University, Haikou, People's Republic of China

Correspondence
Cheng Luo, University of Electronic Science and Technology of China, Second North Jianshe Road, Chengdu 610054, People's Republic of China.
Email: chengluo@uestc.edu.cn

Funding information
CAMS Innovation Fund for Medical Sciences, Grant/Award Number: 2019-I2M-5-039; China Postdoctoral Science Foundation, Grant/Award Numbers: 2021M700852, BX2021078; National Natural Science Foundation of China, Grant/Award Numbers: 61933003, 81901730, 81960249, U2033271; Natural Science Foundation of Sichuan Province, Grant/Award Numbers: 22NSFSC0530, 23NSFSC0016; Shanghai Sailing Program from Shanghai Science and Technology Committee, Grant/Award Number: 22YF1402800; Sichuan Provincial Program of Traditional Chinese Medicine, Grant/Award Number: 2021ZD017

Abstract

Temporal lobe epilepsy (TLE) is the most common type of intractable epilepsy in adults. Although brain myelination alterations have been observed in TLE, it remains unclear how the myelination network changes in TLE. This study developed a novel method in characterization of myelination structural covariance network (mSCN) by T1-weighted and T2-weighted magnetic resonance imaging (MRI). The mSCNs were estimated in 42 left TLE (LTLE), 42 right TLE (RTLE) patients, and 41 healthy controls (HCs). The topology of mSCN was analyzed by graph theory. Voxel-wise comparisons of myelination laterality were also examined among the three groups. Compared to HC, both patient groups showed decreased myelination in frontotemporal regions, amygdala, and thalamus; however, the LTLE showed lower myelination in left medial temporal regions than RTLE. Moreover, the LTLE exhibited decreased global efficiency compared with HC and more increased connections than RTLE. The laterality in putamen was differently altered between the two patient groups: higher laterality at posterior putamen in LTLE and higher laterality at anterior putamen in RTLE. The putamen may play a transfer station role in damage spreading induced by epileptic seizures from the hippocampus. This study provided a novel workflow by combination of T1-weighted and T2-weighted MRI to investigate in vivo the myelin-related microstructural feature in epileptic patients first time. Disconnections of mSCN

implicate that TLE is a system disorder with widespread disruptions at regional and network levels.

KEYWORDS
hippocampus, magnetic resonance image, myelin, structural connectivity, structural covariance, temporal lobe epilepsy

1 | INTRODUCTION

Temporal lobe epilepsy (TLE) is the most common type of intractable epilepsy in adults (Wiebe & Jette, 2012). Although magnetic resonance imaging (MRI) morphometric measures, such as cortical thickness or grey-matter (GM) volume, have demonstrated medial temporal atrophy, cortical thinning and subcortical abnormalities (Caciagli et al., 2017), a few studies found brain myelination alterations in TLE. For example, an earlier histopathological study of surgical specimens reported anomalies of cortical myelinated fibres in TLE (Thom et al., 2000). A recent study has demonstrated atypical morphology of myelinated axons in TLE patients with temporo-polar blurring, using a combination of ex vivo MRI and histological analysis (Garbelli et al., 2012). To date, the noninvasive study of myelin changes in the human brain remains a challenge. Recently, a method based on the ratio of T1-weighted (T1w) and T2-weighted (T2w) magnetic resonance images provides insight in the characterization of microstructural myelination changes underlying brain cortical and subcortical GM and white matter (WM) in vivo (Glasser & Van Essen, 2011). The T1w/T2w ratio, by simultaneously enhancing the sensitivity to myelin signal intensity while reducing the inter-subject signal intensity bias, can be used as a measure for detecting changes in myelination degree associated with diseases (Glasser & Van Essen, 2011). T1w/T2w ratio has been widely applied to study cortical and WM changes in ageing adults, multiple sclerosis and post-traumatic stress disorder (Chao et al., 2015; Granberg et al., 2017).

Studies suggested that TLE may be more adequately described as a disorder with changes in brain network organization (Bernhardt et al., 2015). Exploring why and how network changes in TLE provided a promising new avenue in the investigation of network mechanisms in epilepsy (Royer et al., 2022). Due to high dimensional of brain network, a formal framework to quantify topological feature of complex network may contribute to provide clinically relevant measures in epilepsy. Several studies have used network-based measures, in particular, metrics capturing global and local efficiency, to increase understanding of dysfunction in TLE, primarily in regard to cognitive phenotyping, localization of the epileptogenic zone, and the prediction of postoperative outcome (Lariviere, Bernasconi, et al., 2021). The study of network mechanisms promises to a better understanding of dysfunction in TLE.

Covariance of structural MRI markers among regions, termed as structural covariance network (SCN), can characterize structural brain organization by identifying interregional covarying. A recent ENIGMA-Epilepsy study of SCN derived morphological measures found increased clustering and path length in orbitofrontal and temporal regions in TLE, indicating a shift towards network regularization (Lariviere, Rodriguez-Cruces, et al., 2021). In addition, increased path length and clustering has been observed in both cortical network and limbic network in TLE (Bernhardt et al., 2011; Bernhardt et al., 2016). However, it is still unclear whether the topological properties of the myelination SCN are distinct between TLE and healthy controls.

In this study, we applied the T1w/T2w analysis workflow to investigate in vivo the microstructural feature of brain tissue in a cohort of patients with left TLE, right TLE, and healthy controls. Subsequently, we employed region of interest (ROI) analysis for the ROI-wise estimation of T1w/T2w in cortical GM, subcortical GM and WM. To evaluate the synchronous changes of T1w/T2w across ROIs, we built a SCN by calculating the correlations between any two ROIs across subjects in each group. We compared differences in the connections and topological properties of the SCN among the left TLE, right TLE, and healthy controls. Finally, we investigated the longitudinal changes of T1w/T2w using another longitudinal sample with anterior temporal lobectomy (ATL) including post-ATL TLE patients.

2 | MATERIALS AND METHODS

2.1 | Participants

This study included 42 left TLE patients (LTLE group: 15 females, age = 25.29 ± 7.96); 42 right TLE (RTLE group: 18 females, age = 26.96 ± 8.33); and 41 healthy controls (HC group, 25 females, age = 29.37 ± 10.63). Patients were selected from the TLE database in West China Hospital, Chengdu, China. All patients were diagnosed with TLE according to the International League Against Epilepsy (Fisher et al., 2017) Classification Schemes of Epileptic Seizures and Epilepsy Syndromes. The inclusion criteria were as follows: (1) patients with MTLE; (2) normal MRI or MRI evidence of hippocampal sclerosis (HS) ipsilateral to the lateralization by EEG; (3) no evidence of bilateral HS or of a secondary extrahippocampal lesion that may contribute to seizures; and (4) underwent both T1-weighted and T2-weighted MRI scans. The exclusion criteria included: (1) patients with any other neurological disorder, psychiatric disorder, or serious systematic disease; (2) with alcohol or other substance abuse. All participants were right handedness. There was no significant difference in the subject age or gender among the three groups ($p > .05$) (Table 1). This study was approved by the local ethics committee and informed consent was obtained from all subjects. Then, 10 of the 84 patients have been

TABLE 1 Demographic and clinical variables

	LTLE ($N = 42$)	RTLE ($N = 42$)	HC ($N = 41$)	*p*-Value
Gender (female)	15	18	25	.060[a]
Age (years)	25.29 ± 7.96	26.96 ± 8.33	29.37 ± 10.63	.122[b]
duration (years)	11.61 ± 8.45	11.22 ± 8.69	-	.837[c]
Handedness (right)	42	42	41	-
Seizure type (FS/FS, sGTCS)	16/26	16/26	-	-
Seizure frequency (daily/weekly/monthly/yearly)	5/20/16/1	5/15/18/4	-	-
History of febrile convulsions (yes)	17	20	-	-
MRI finding (MTS/negative)	29/13	40/2	-	-
Number of current AEDs (0/1/2/3/4)	2/11/17/11/1	1/17/17/5/2	-	-

Abbreviations: AEDs, antiepileptic drugs; FS, focal seizures; HC, healthy controls; LTLE, Left TLE; MTS, mesial temporal sclerosis; RTLE, right TLE; sGTCS, secondary generalized tonic–clonic seizures; TLE, temporal lobe epilepsy.
[a]Chi-square test.
[b]ANOVA.
[c]Two-sample *t* test.

previously reported in our prior article which explored the dynamic changes of WM microstructure measured by diffusion tensor imaging in mesial TLE patients following ATL (Li et al., 2019). Different than the previous research, the current study investigated abnormalities of myelin in TLE by using T1- and T2-weighted MRI data.

2.2 | Image acquisition

High-resolution T1-weighted images were acquired using spoiled gradient recalled sequence on a 3 T MRI system (Tim Trio; Siemens, Erlangen, Germany) with an eight-channel head coil at West China Hospital. The main parameters included: repetition time (TR) = 1900 ms; echo time (TE) = 2.26 ms; flip angle (FA) = 9°, field of view (FOV) = 256 × 256 mm^2; voxel size = 1.0 × 1.0 × 1.0 mm^3, 176 slices. T2-weighted images were acquired using a turbo spin echo sequence (TR: 6100 ms; TE: 97 ms; FA: 120°; FOV: 230 mm; voxel size = 0.6 × 0.6 × 3.9 mm^3; 35 slices).

2.3 | Data processing

A flowchart is provided in Figure 1. T1w and T2w images were preprocessed and combined, using a dedicated workflow outlined in previous studies (Ganzetti et al., 2014). This process included bias correction and intensity calibration on each of the T1w and T2 images and subsequent calculation of the ratio between the two images. In detail, each subject's T2w image was co-registered to the T1w images using a rigid-body transformation. Second, bias correction was conducted on the T1w and T2w images separately. After correction for intensity nonuniformity, the T1w and T2w images were processed to standardize their intensity using a linear scaling procedure (Ganzetti et al., 2014). Subsequently, the ratio was calculated to obtain the T1w/T2w image. Finally, the T1w/T2w image was normalized to the Montreal Neurological Institute space. The entire T1w/T2w image processing was performed using the MR Tool-Multimodal Mapping (Release 1.3.1, http://www.bindgroup.eu/wp-content/uploads/2017/02/mrtool-v1.3.1.zip), a MATLAB-based toolkit requiring SPM version 12 (http://www.fil.ion.ucl.ac.uk/spm/software/spm12/).

2.4 | Tissue and ROI analysis

The GM and WM masks were defined based on the tissue probability map provided in SPM12 (threshold = 50%). The average T1w/T2w intensity within GM and WM masks was calculated. To gain further insight to the precise regions, the WM component was refined into 48 ROIs (21 bundles in each hemisphere and 6 commissure bundles) using the JHU ICBM-DTI-81 WM atlas (Mori et al., 2008), and the GM cortical (96 ROIs) and subcortical (16 ROIs) components were refined based on the Harvard-Oxford GM atlas (Desikan et al., 2006). The average T1w/T2w intensity value was extracted from each ROI. ANCOVA was performed to examine the group difference among the LTLE, RTLE, and HC, with age and gender as the covariates. The *p* value <.05/160 was considered significant for the multiple comparison correction (Bonferroni correction). In addition, the post hoc tests were performed for the comparisons between any two groups.

2.5 | Correlation analysis between imaging parameters and clinical variables

ROI-wise T1w/T2w intensity was extracted for regions with significant group difference. As clinical variables were not normally distributed, Spearman correlation analysis was performed between regional T1w/T2w intensity and clinical variables including the age of onset and seizure frequency.

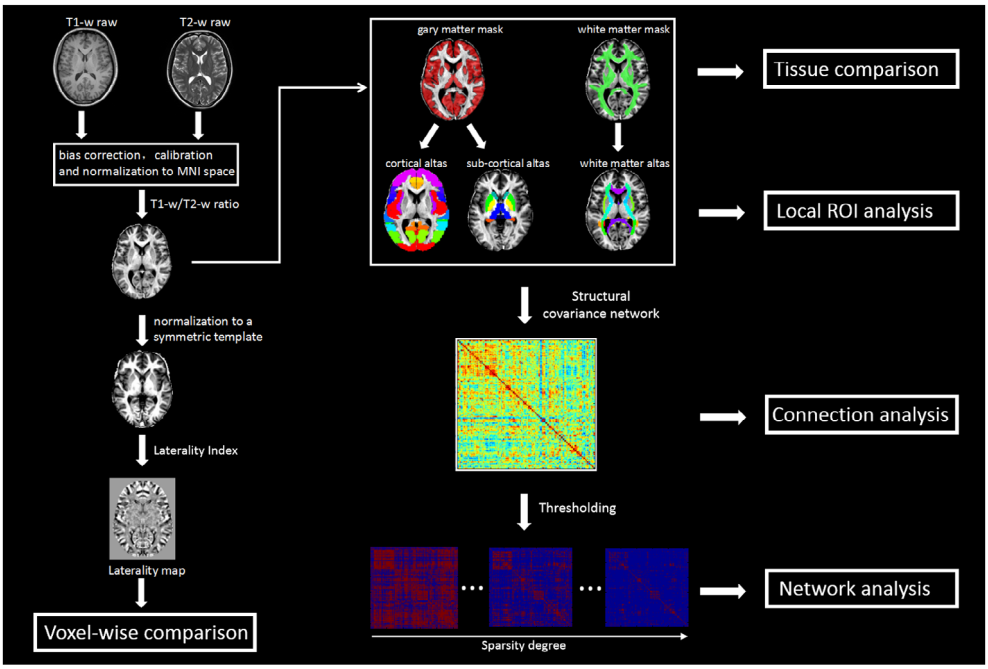

FIGURE 1 The flowchart of data processing. First, the T1w and T2w images were pre-processed by the bias correction, intensity calibration and normalization using the MR Tool-Multimodal Mapping (http://www.bindgroup.eu/wp-content/uploads/2017/02/mrtool-v1.3.1.zip) implemented in SPM12 (http://www.fil.ion.ucl.ac.uk/spm/software/spm12/) to obtain the T1w/T2w map. Second, the averaged T1w/T2w value was extracted from each region of interest (ROI) of JHU ICBM-DTI-81 white-matter atlas and the Harvard-Oxford grey-matter atlas. Third, the myelination structural covariance network (mSCN) was built according to the strategy of the T1w/T2w structural covariance network. The connection of the mSCN was defined as the Pearson's correlation coefficient across subjects between each pair of ROIs. Hence, the interregional correlation matrix ($N \times N$, $N = 160$) was obtained to represent the similarity or synchronized co-variations in T1w/T2w. Next, we used graph theory to characterize the mSCN attributes. Finally, the laterality analysis was performed by first co-registering the T1w/T2w map into a symmetric template. Subsequently, we calculated the laterality index (LI) for each homotopic voxel and thus obtained a laterality map for each subject

2.6 | Myelination SCN analysis

Based on T1w/T2w intensity, the myelination SCN (mSCN) was built as described in the previous study by Melie-Garcia (Melie-Garcia et al., 2018). Previous studies have found that TLE patients showed structural abnormalities involving the cortical and subcortical GM as well as WM (Li et al., 2019; Li et al., 2021). As such, a whole brain mSCN consisting of 160 regions within WM and GM was constructed in this study. Based on JHU ICBM-DTI-81 WM atlas and the Harvard-Oxford GM atlas, the whole brain was parcellated into 48 WM ROIs and 112 GM ROIs. The T1w/T2w data matrix was $M \times N$, where M is the number of subjects and N represents the ROI number ($N = 160$ in the current study). A linear regression was conducted on the T1w/T2w data matrix to remove the effects of gender, age, and age^2 (Melie-Garcia et al., 2018). The connection of the mSCN was defined as the Pearson's correlation coefficient across subjects between each pair of ROIs. Hence, the interregional correlation matrix ($N \times N$, $N = 160$) was obtained to represent the similarity or synchronized co-variations in T1w/T2w. To avoid the influence of the weak correlations, one sample t test was performed to determine the significant correlation ($p < .05$, FWE correction). To compare the group differences in the connection strength, a permutation test was performed (Palaniyappan et al., 2015). In brief, we randomly assigned the group labels across subjects and re-generated the mSCN, which was repeated 100,000 times. We computed the difference of each connection between the two random groups and generated a distribution of the null hypothesis of equality in connection strength between groups. Based on the location of the real group difference of connection strength within the distribution of the null hypothesis, a p value was calculated for each connection.

Next, we used graph theory to characterize the mSCN attributes. The sparse binary graphs were created using a range of sparsity degrees that varied from 0.1 to 0.4 with a step of 0.02 (Melie-Garcia et al., 2018). Subsequently, the network attributes, including clustering coefficient, characteristic path length, and global and local efficiency, were computed for the LTLE, RTLE, and HC groups for each sparsity threshold. The formula and interpretations of graph measures can be found in prior research (Rubinov & Sporns, 2010). Finally, we calculated the area under the curve (AUC) for each network metric. The AUC metric can provide an integrated scalar for brain network topological characterization independent of a single threshold selection (Lei et al., 2015). Statistical significance of the group differences was assessed using the permutation test, with a p-value <.05 (Palaniyappan et al., 2015). In detail, group labels were randomly assigned across all subjects and the mSCN attributes of each group was recalculated 10,000 times. The permutation processing allows for

nonparametric estimation of the null distribution for the difference between any two groups.

2.7 | Laterality analysis

Lateralization is an obvious feature in brain structural damage of TLE. Accumulated evidence has suggested different alterations of GM volume (Liu et al., 2016), cortical thickness (Liu et al., 2016), and connectivity (de Campos et al., 2016) between left TLE and right TLE. To further examine the impact of the seizure side on the myelination, laterality analysis was performed here. Due to the differences of geometric configuration between cerebral hemispheres, each subject's T1w/T2w images were nonlinearly registered into a symmetrical template (Zuo et al., 2010). Referring to previous studies (Zuo et al., 2010), we created the symmetrical template using the following steps. First, all subjects' normalized T1w/T2w images were averaged to obtain a group mean template. Then, the mean group template was left-to-right flipped and re-averaged to create a symmetrical template (Zuo et al., 2010). In the symmetrical brain space, we calculated the laterality index (LI) for each homotopic voxel (Agcaoglu et al., 2015), that is:

$$LI_{LR} = \frac{Intensity_{left} - Intensity_{right}}{Intensity_{left} + Intensity_{right}}$$

where $Intensity_{left}$ represents the left T1w/T2w intensity and $Intensity_{right}$ represents the right T1w/T2w intensity for each homotopic voxel.

By the LI calculation of each homotopic voxel, we obtained a laterality map for each subject. Voxel-wise ANCOVA was performed on the laterality maps to compare the differences among the LTLE, RTLE, and HC, after controlling for the effects of gender and age. Multiple comparisons correction was performed using cluster-wise false discovery rate (FDR) correction (corrected $p < .05$) (Chumbley & Friston, 2009).

3 | RESULTS

3.1 | Tissue and ROI analysis

Consistent with a previous study (Ganzetti et al., 2015), tissue comparison confirmed that WM had higher T1w/T2w intensity than GM (Figure 2a). In addition, we found T1w/T2w reductions in TLE for GM and WM, compared to controls (Figure 2a).

We then focused our investigation on specific brain regions within the WM and GM including subcortical and cortical regions. After the multiple comparison correction, a total of 20 GM regions and 4 WM regions exhibited significant group differences among the LTLE, RTLE, and HC groups. GM subcortical ROI comparisons showed that, compared with HC, both LTLE and RTLE groups had decreased T1w/T2w intensity in the left amygdala, left thalamus and bilateral hippocampus (Figure S1, Table S1), with more severe reduction in the ipsilateral hippocampus (Figure 2b,c) in each patient group. Cortical ROI analysis found that compared with HC, both TLE groups had lower T1w/T2w in the temporal lobes (bilateral temporal pole [TP], left anterior superior temporal gyrus, right posterior temporal fusiform cortex, left posterior middle temporal gyrus, left anterior inferior temporal gyrus, left posterior parahippocampal gyrus [PPHIP]), frontal lobes (left pars triangularis of inferior frontal gyrus [TriIFG], bilateral middle frontal gyrus, left subcallosal cortex [SCC], and left frontal

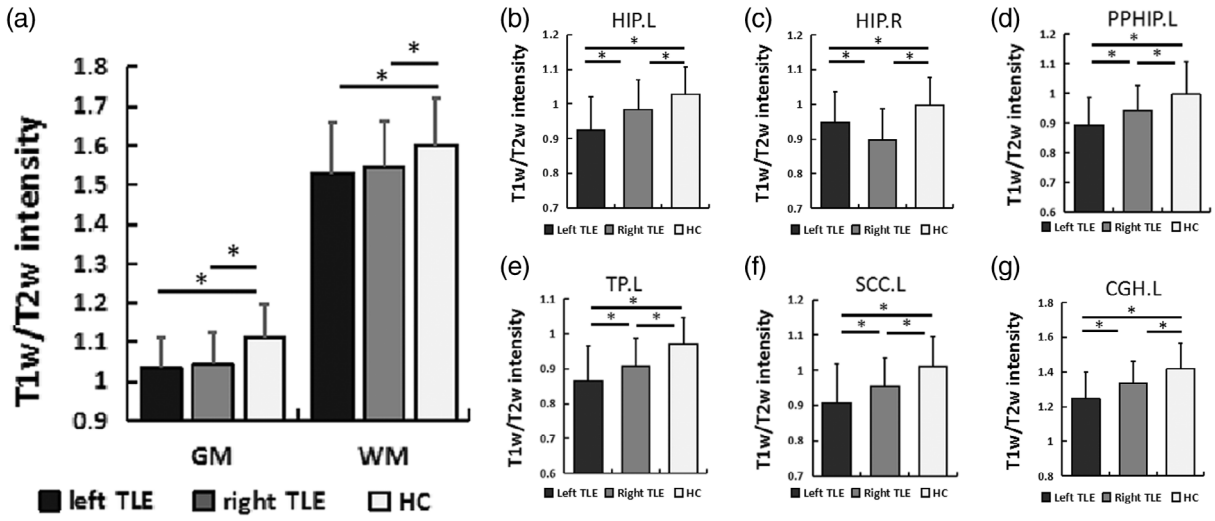

FIGURE 2 Differences of T1w/T2w intensity among the left temporal lobe epilepsy (TLE), right TLE, and HC in (a) GM and WM masks, (b) left HIP, (c) right HIP, (d) left CGH, (e) left TP, (f) left SCC, and (g) left PPHIP. The $p < .05/160$ was considered significant for the multiple comparisons correction (Bonferroni correction). The error bars represent standard deviations. CGH, cingulum adjoining the hippocampus; GM, grey matter; HC, healthy controls; HIP, hippocampus; PPHIP, posterior parahippocampal gyrus; SCC, subcallosal cortex; TLE, temporal lobe epilepsy; TP, temporal pole; WM, white matter. * represents $p < .05$, Bonferroni correction

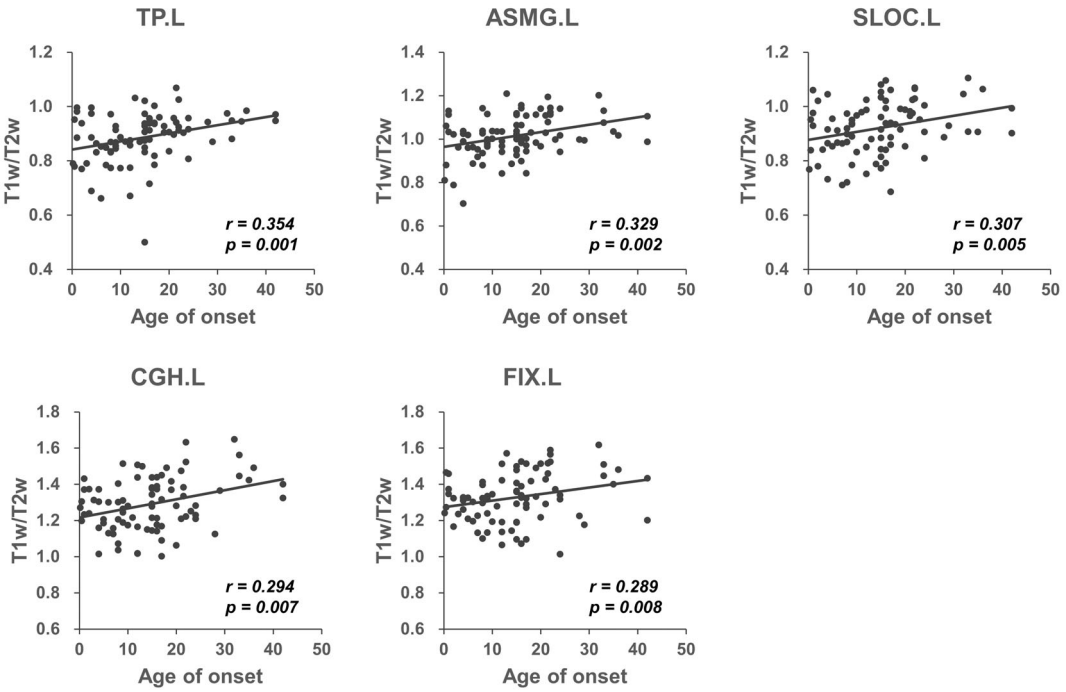

FIGURE 3 Correlation between T1w/T2w and age of onset. ASMG.L, left anterior supramarginal gyrus; CGH.L, left cingulum adjoining the hippocampus; FIX.L, left fornix body; SLOC, left superior lateral occipital cortex; TP.L, left temporal pole

pole), occipital lobes (left superior lateral occipital cortex [SLOC] and right occipital pole), parietal (left anterior supramarginal gyrus [ASMG]) and insular lobes (right insula) (Figure S3, Table S2). Additionally, the LTLE showed more severe decreases in the left PPHIP (Figure 2d), left TP (Figure 2e), and left SCC (Figure 2f), compared with RTLE. WM ROI analysis indicated lower T1w/T2w in bilateral cingulum adjoining the hippocampus (CGH) and fornix body (FIX) in both TLE groups (Figure S2, Table S3). In left CGH, the LTLE exhibited reduced T1w/T2w intensity compared to the RTLE (Figure 2g). Power analyses were conducted using the G × Power 3.1.9.2 (http://www.gpower.hhu.de/) to estimate the effect size and statistical power for these group differences in T1w/T2w intensity (Table S4).

We also conducted the group comparisons among the three groups at the voxel-wise. Consistent with the results at the ROI-wise, these regions exhibiting significant differences among the three groups were mainly located at the bilateral hippocampus, bilateral temporal areas and FIX (Figure S4 and Table S5) after correcting the multiple comparisons by Gaussian random field theory (corrected $p < .05$).

3.2 | Correlation between T1w/T2w and clinical variables

A total of 24 ROIs showing significant group difference was included in the correlation analysis. We found that the age of onset was positively correlated with the T1w/T2w intensity in the left TP ($r = .354$, $p = .001$); left ASMG (.329, $p = .002$); left SLOC ($r = .307$, $p = .005$); left CGH ($r = .294$, $p = .007$); and left FIX ($r = .289$, $p = .008$) (Figure 3) by FDR correction. In addition, voxel-wise analysis also indicated significant correlation between the age of onset and the T1w/T2w intensity in regions including the left TP, temporal, and occipital cortex (Figure S5) after correcting the multiple comparisons by Gaussian random field theory (corrected $p < .05$).

3.3 | mSCN analysis

The edges of the mSCN indicated significant correlations between T1w/T2w measures of specific ROIs across subjects. By comparing patients and healthy controls, the edges can be described as decreased connections (ROI–ROI correlation was significantly lower in patients compared with controls) and increased connections (ROI–ROI correlation was significantly higher in patients compared with controls) by the permutation test (Figure 4a). In total, compared with HC, the LTLE group showed more changed connections than RTLE (59 vs. 35) (Table 2). Furthermore, there were more increased connections than decreased connections (29 vs. 19) in the LTLE group, while there were more decreased connections than increased connections (20 vs. 5) in the RTLE group (Table 2). In both LTLE and RTLE groups, there were more extensive changes in the cortical ROI to cortical ROI connection pattern, compared with other connection patterns (Table 2), such as subcortical ROI to subcortical ROI connection or WM ROI to WM ROI connection. In addition, there were more increased cortical-to-cortical connections in LTLE than RTLE (29 vs. 5), especially for the frontotemporal connectivity.

Graph theory analysis revealed that compared with HC, only the LTLE group had higher characteristic path length and lower global

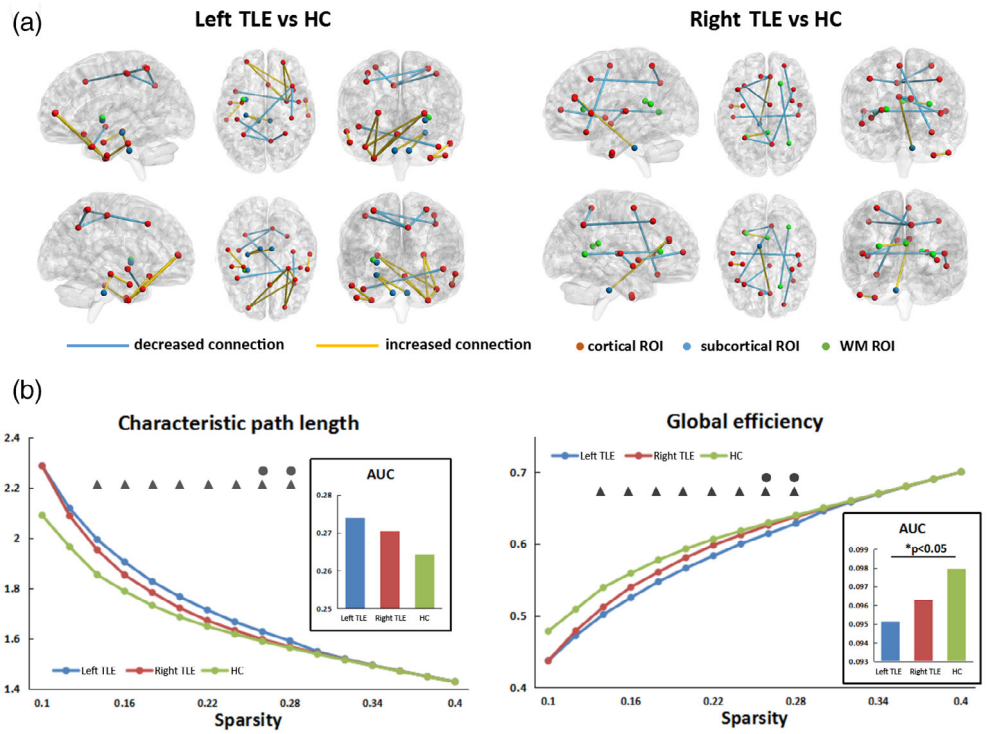

FIGURE 4 Changes of the myelination structural covariance network in left temporal lobe epilepsy (TLE) and right TLE. (a) By comparing patients and HCs, the edges can be described as decreased connections (region of interest [ROI]–ROI correlation was significantly lower in patients compared with controls) and increased connections (ROI–ROI correlation was significantly higher in patients compared with controls). (b) Differences of attributes in the structural covariance network among the left TLE, right TLE, and HC. The triangles represent significant differences between left TLE and HC ($p < .05$). The circles represent significant differences between left TLE and right TLE ($p < .05$). HC, healthy controls; TLE, temporal lobe epilepsy

TABLE 2 Decreased connections and increased connections of myelination structural covariance network in left TLE and right TLE

	Decreased connection		Increased connection	
Connection	**Left TLE**	**Right TLE**	**Left TLE**	**Right TLE**
Cortical ROI to cortical ROI connection	19	20	29	5
Subcortical ROI to subcortical ROI connection	1	0	3	2
WM ROI to WM ROI connection	2	3	0	2
Cortical ROI to subcortical ROI connection	2	1	0	2
Cortical ROI to WM ROI connection	3	0	0	0
Subcortical ROI to WM ROI connection	0	0	2	0
Total	25	24	34	11

Abbreviations: ROI, region of interest; TLE, temporal lobe epilepsy; WM, white matter.

efficiency for a range of sparsity threshold from 0.14 to 0.28 (all *p*s <.05 by permutation test) (Figure 4b). Moreover, the comparisons between two patient groups showed higher characteristic path length and lower global efficiency in LTLE at the sparsity of 0.26 and 0.28 ($p < .05$) (Figure 4b). In addition, the AUC analysis showed that only the LTLE group exhibited a significant decrease ($p < .05$) in the AUC of global efficiency and a marginally significant increase ($p = .050$) in the AUC of characteristic path length, compared with HC (Figure 4b). There was no significant difference among the healthy controls, LTLE and RTLE group, in terms of clustering coefficient and local efficiency (all *p*s >.05).

3.4 | Hippocampus-associated SCN analysis

We examined the covariance connectivity with the seed ROI of lesioned hippocampus. We calculated the Fisher's z score of Pearson's correlation coefficient between the seed ROI (i.e., the lesioned hippocampus) and other 159 ROIs and then averaged. The permutation test was used to compare the differences among the LTLE, RTLE, and HC groups. We found that compared with the HC, only LTLE showed significantly decreased lesioned hippocampal covariance connectivity by the permutation test ($p = .003$).

To examine the potential effect of lesioned hippocampus on the mSCN topology, we re-built covariance network using all regions except the lesioned hippocampus (i.e., removing the lesioned hippocampus and its connections from the covariance network). We found that after removing the lesioned hippocampus and its connections to other regions, the mSCN no longer showed significant group difference, in terms of global efficiency or characteristic path length, between the LTLE and HC groups ($p > .05$). This suggested that the decreased efficiency of whole brain network in LTLE may be due to the lesioned hippocampus and its connections to other regions.

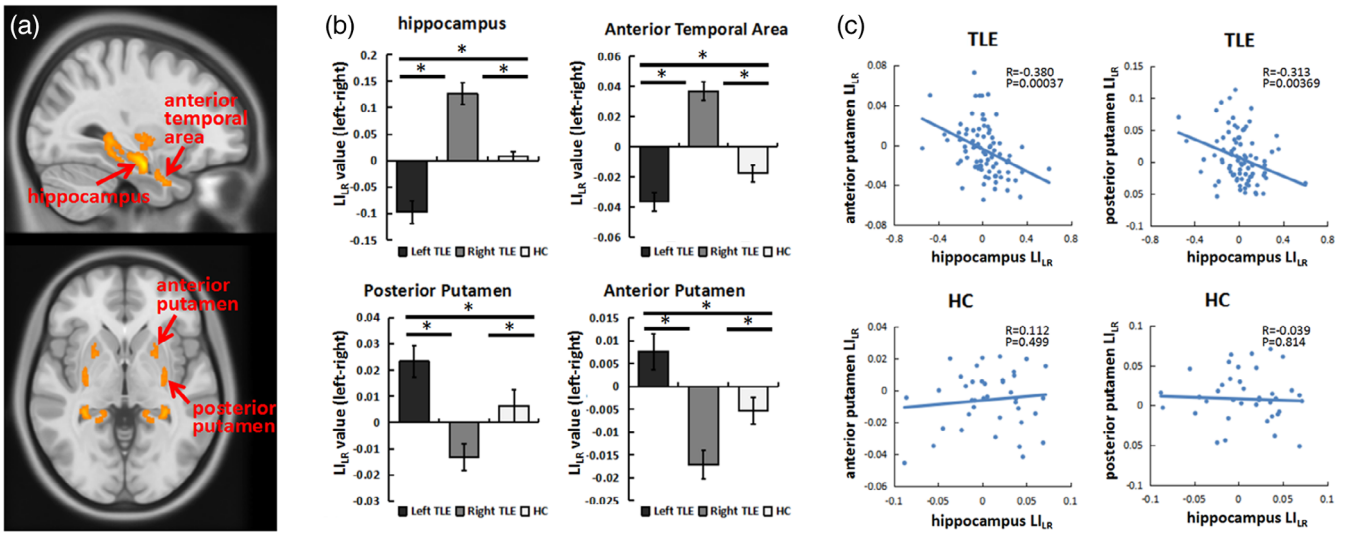

FIGURE 5 Results of laterality analysis in TLE. (a) Brain regions with significant differences of LILR maps among the left TLE, right TLE, and HC groups by ANCOVA ($p < .05$, false discovery rate [FDR] correction). (b) Altered LILR in the hippocampus and putamen in left TLE and right TLE compared with HC by post hoc analysis. (c) A significant correlation between hippocampal LILR and anterior and posterior putamen's LILR in a cohort of all TLE patients but not in HC. HC, healthy controls; LI, laterality index; TLE, temporal lobe epilepsy. * represents $p < .05$, Bonferroni correction

3.5 | Laterality analysis

3.5.1 | Discovery findings

The ANCOVA on the LI_{LR} maps showed significant differences among the LTLE, RTLE, and HC groups in anterior and posterior putamen, hippocampus and anterior temporal area ($p < .05$, FDR correction) (Figure 5a). The post hoc tests revealed that there was decreased LI_{LR} in LTLE and increased LI_{LR} in RTLE compared with HC (*p*s <.05, Bonferroni correction) (Figure 5b). In detail, one-sample *t* tests showed that the laterality of the anterior temporal area was significantly different from zero in all three groups (corrected *p*s <.05). The laterality of the hippocampus and posterior putamen existed in LTLE and RTLE (corrected *p*s <.05) but not in the HC. The laterality of the anterior putamen existed only in the RMTL (corrected $p < .05$). Due to the LI_{LR} calculation (left–right), both LTLE and RTLE exhibited a consistent decrease of T1w/T2w LI_{LR} at the ipsilateral hippocampus. Except for the hippocampus and anterior temporal area, both TLE groups showed a T1w/T2w LI_{LR} decrease at the contralateral putamen (all *p*s <.05) (Figure 5b).

As there are structural connections between the hippocampus and putamen, we further investigated whether a damaging synchronization between the hippocampus and putamen exists. We found a significant Pearson's correlation between hippocampal LI_{LR} and anterior and posterior putamen LI_{LR} in a cohort of all TLE patients (anterior putamen: $R = -.380$, $p < .001$; anterior putamen: $R = -.313$, $p = .004$) but not in the HC (anterior putamen: $R = .112$, $p = .499$; anterior putamen: $R = -.039$, $p = .814$) (Figure 5c).

In addition, we observed different alterations between putamen anterior and posterior regions in LTLE and RTLE. To better clarify the laterality changes in the putamen and perform a directed comparison between LTLE and RTLE, we redefined the laterality measure as the following equation:

$$LI_{IC} = \frac{Intensity_{ips} - Intensity_{con}}{Intensity_{ips} + Intensity_{con}}$$

where $Intensity_{ips}$ represents the ipsilateral T1w/T2w intensity and $Intensity_{con}$ represents the contralateral T1w/T2w intensity for anterior and posterior putamen. A high value of the LI_{IC} represented a high T1w/T2w intensity on the contralateral putamen. We identified a significant interaction effect ($F = 4.26$, $p < .05$) between the side of epileptic focus (left or right) and the LI_{IC} of the putamen anterior or posterior (Figure S6) using the repeated measured ANOVA. Specifically, the LTLE showed a higher laterality at the posterior putamen, while the RTLE exhibited a higher laterality at the anterior putamen (Figure S6).

3.5.2 | ATL influence on the putamen

To further investigate the ATL influence on the putamen, we focused on the following questions: Are there longitudinal changes in the LI_{IC} of putamen after ATL? If so, how does the T1w/T2w of bilateral putamen change? We measured the longitudinal changes in another longitudinal cohort of 14 refractory TLE patients who received ATL and included both pre-ATL and post-ATL MRI data (see Supplementary Table S6 for details). Paired t-tests indicated increased LI_{IC} in both anterior ($T = 3.20$, $p = .007$) and posterior putamen ($T = 8.47$, $p < .001$) in the TLE patients after ATL (Figure S7). Subsequently, to

further determine which putamen subregions T1w/T2w changes contribute to the increased LI_{IC}, we compared the longitudinal T1w/T2w intensity alterations between pre-ATL and post-ATL in ipsilateral and contralateral putamen subregions. We found increased T1w/T2w intensity only in the ipsilateral putamen after ATL (ipsilateral anterior putamen: $T = 2.91$, $p = .012$; ipsilateral posterior putamen: $T = 5.92$, $p < .001$) (Figure S8).

4 | DISCUSSION

This study used the T1w/T2w ratio to measure in vivo the brain microstructural changes in a large cohort of TLE patients, which allowed separate baseline analysis of LTLE and RTLE. Another cohort of TLE patients undergoing ATL surgery enables a further validation study of longitudinal changes induced by the ATL. First, compared to the HC, both LTLE and RTLE groups showed decreased T1w/T2w in cortical areas (mainly in frontotemporal regions), subcortical regions (hippocampus, amygdala and thalamus) and WM (CGH and FIX). Moreover, LTLE presented with lower T1w/T2w in left medial temporal region, compared to RTLE. Second, the mSCN analysis indicated that compared to HC, both LTLE and RTLE groups had extensive changes of cortex–cortex connections. However, LTLE presented with more increased connections than RTLE. In addition, only the LTLE group exhibited a significant decrease in the global efficiency of mSCN compared with HC. Third, the two TLE groups showed altered laterality of T1w/T2w in the hippocampus and putamen. Moreover, the T1w/T2w at the two regions exhibited a negative correlation in the patient cohort. Additionally, we found that the LTLE showed a higher laterality at the posterior putamen, where the RTLE exhibited a higher laterality at the anterior putamen. Lastly, we found increased T1w/T2w only in the ipsilateral putamen following the ATL.

4.1 | T1w/T2w intensity decreases in cortical, subcortical regions, and WM in TLE

The present findings provided brain microstructural changes of T1w/T2w ratios in TLE, using a combination of two MRI measures (Ganzetti et al., 2014). Across the two groups of TLE and HC, the comparisons using WM and GM as ROIs suggested a global reduction of T1w/T2w intensity in TLE. This result is consistent with current studies suggesting that TLE is a system-level disorder, with both GM and WM disruptions as the foundation for the clinical outcome of the pathology (Bernhardt et al., 2013). Regarding structural impairments in GM cortices, we found prominent alterations in TLE patients to be localized in the frontal and temporal lobes, which were consistent with previous studies revealing that abnormalities of frontal-temporal networks may be linked to cognitive impairments and pathological outcomes in TLE (Hwang et al., 2019). Regarding subcortical structures, we found T1w/T2w decreases in the hippocampus, amygdala and thalamus. The results were consistent with cumulative evidence indicating a key role of a thalamotemporal network in the pathologic alterations of TLE (Guye et al., 2006). Regarding the WM results, the current study identified a reduction of T1w/T2w intensity in the WM tracts of CGH and FIX in the TLE patients. Several studies have also reported consistent WM aberrations in hippocampal WM pathways (Winston et al., 2014). Previous studies using diffusion tensor imaging have observed widespread microstructural organizational changes, such as reduced fractional anisotropy (FA), which is possibly linked to myelination alterations (Reyes et al., 2019). The current study demonstrated that earlier ages of onset associated with more reduction in T1w/T2w intensity. Previous work has also reported aberrant myelin content in children with epilepsy (Drenthen et al., 2019). These findings provided evidences on the relationship between pathophysiology of epilepsy and myelin abnormalities (Drenthen et al., 2020). In brief, the observed changes in T1w/T2w intensity further provided evidences supporting microstructure alterations in TLE by an advanced method in multimodal neuroimaging.

4.2 | mSCN is distinct in left and right TLE

The SCN method has been widely used to investigate the concurrent changes of brain structures (i.e., cortical thickness) in normal and pathological brain (Alexander-Bloch et al., 2013). To characterize the concurrent changes in T1w/T2w across brain anatomical structures in vivo, this study built an mSCN by calculating the synchronicity of the variations in T1w/T2w between anatomical regions. The T1w/T2w covariance network pointed to more severe and more extensive changes in LTLE than RTLE. Such distinct network alterations agree with several structural studies of GM and WM (Besson et al., 2014; Keller et al., 2002). For example, morphological analysis on GM volume showed a stronger reduction in patients with left-sided seizure origin (Bonilha et al., 2007). Investigations of FA in WM tracts identified more widespread deficits in LTLE (Pustina, Doucet, et al., 2015). Focke et al. also found that the WM tract of arcuate fasciculus was more affected in LTLE (Focke et al., 2008). Wang et al. reported aberrant topological patterns of metabolic covariance networks in TLE (Wang et al., 2019). In addition, Campos et al. indicated that LTLE had a more intricate bilateral bi-hemispheric dysfunction compared to RTLE using resting-state fMRI (de Campos et al., 2016). In total, our findings identified a distinct pathological network of T1w/T2w, which exhibited more connectome alterations in LTLE than RTLE, supporting previous suggestions that LTLE is a more severe network disease than RTLE (Besson et al., 2014).

The topological properties of the SCN were also altered in LTLE. The "characteristic path length" was statistically higher in LTLE. The increased "characteristic path length" was accompanied by a decreased "global efficiency" in principle. According to the graphical theory, higher "characteristic path length" represents higher "wiring cost" for information communication within the network. Additionally, human brain studies also demonstrated that the interpretation is reasonable. For example, Melie-Garcia et al. reported an increasing characteristic path length in an old-age group compared to young-age subjects, suggesting that worse network efficiency is related to poor

performances in older subjects (Melie-Garcia et al., 2018). We observed worse brain network efficiency in LTLE patients, suggesting abnormal brain topological organization in LTLE. These findings provided further support for the hypothesis that abnormalities of brain network efficiency in LTLE may be more serious than in RTLE (Kemmotsu et al., 2011). The worse connectivity/network may indicate that the neuropathological damage in LTLE is more likely to affect or spread to other areas, further showing abnormalities at the global-level. But it needs to be confirmed using longitudinal samples.

4.3 | Laterality of T1w/T2w analysis: The putamen may play a crucial role in controlling epileptic seizures

Asymmetry is used for pathological detection for several reasons. First, the degree of asymmetry is commonly reviewed by expert radiologists who visually inspect the neuroimaging data in search of pathology. Second, asymmetry measurement can reduce confounding factors from differences in diseases, scanner parameters, and neuroimaging modalities, by using each subject as a control for itself. Third, previous studies have shown that asymmetric measures are more sensitive to pathological characterization than raw voxel values (Pustina, Avants, et al., 2015).

In TLE, previous studies have shown asymmetric atrophy in mesial temporal structures and asymmetric reduction of glucose metabolism in the temporal lobes (Pustina, Avants, et al., 2015). A recent study found that TLE patients showed greater GM volume in contralateral hippocampus and subfields, indicating volumetric asymmetry in TLE (Shah et al., 2019). Resting-state fMRI studies also reported decreased ipsilateral functional connectivity within the mesial temporal lobes in TLE (Bettus et al., 2010). Consistent with these findings, we observed asymmetric anomalies related to pathological changes in the hippocampus, using the ratio of T1w/T2w images. In addition, the current study found asymmetric alteration of T1w/T2w in the putamen in TLE. The putamen, as a subcortical region, is a principal anatomical component of the basal ganglia, which receives inputs from the cortical areas and sends information back to the cortex via the thalamus (Duan et al., 2015). The basal ganglia show intimate structural connections with the brain limbic system, especially the hippocampus (Bland, 2004). Reduction of GM volume has also been reported in the basal ganglia, including the putamen in TLE patients (Kim et al., 2016). Additionally, aberrant functional connectivity in the basal ganglia and hippocampus has been noted previously in TLE (Haneef et al., 2014). Furthermore, we found that the T1w/T2w values of the putamen negatively correlated with that of the hippocampus. According to the structural connection and functional association between the hippocampus and putamen, we hypothesized that the putamen may play a transfer station role in damage spreading induced by epileptic seizures from the hippocampus. The hypothesis was further supported by the finding that the T1w/T2w of the putamen increased after the ATL. These results are consistent with previous studies reporting that the basal ganglia play an important role in control of the epileptic activity through the brain (Dreifuss et al., 2001). However, we found the myelination improvement only appeared in the ipsilateral putamen, which may suggest a lateralization effect of the putamen improvement induced by the ATL. These findings may guide the development of new intervention targets or treatment strategies that may modulate morphological reorganization in specific subcortical nuclei. In addition, we found different patterns of T1w/T2w laterality in putamen subregions between LTLE and RTLE, revealed by a higher laterality at the posterior putamen in the LTLE, but a higher laterality at the anterior putamen in the RTLE. This finding provided evidence for identifiable differences of myelination damages in the putamen between LTLE and RTLE.

4.4 | Limitations

The current study had several limitations. First, the present study used the T1w/T2w ratio method to characterize the brain changes of myelination. Other measures of myelination mapping, such as magnetization transfer ratio (MTR), should be investigated in the future work, although previous studies have demonstrated a high degree of correlation between MTR and T1w/T2w ratio (Vandewouw et al., 2019). Second, myelination largely contributes to the ratio of the T1w/T2w images; however, some factors, including inflammation, edema, metabolism, atrophy, or iron accumulation, may also contribute to the T1w/T2w signals (Ganzetti et al., 2014). The T1w/T2w ratio used in the current study is an estimate of T1w/T2w, not a fully quantitative measure of it (i.e., quantitative T1 and T2 relaxometry was not performed). Third, the cohorts of patients before and after ATL surgery enable a baseline comparison and a further investigation of longitudinal changes following surgery. Not all patients underwent the ATL surgery. In addition, the dynamic brain changes should be further investigated on data from multiple postoperative time points. Disease duration and medication use may also affect the secondary changes in the T1/T2 ratio map. The current sample size is relative small. A larger sample size with greater statistical power is needed to further verify the significance of the group differences. In addition, the neuropsychological assessments were not evaluated; thus, we could not assess the associations between behaviour variables and brain changes. As the SCN is built based on the group population, which limits the estimation for the association between the myelination SCN and clinical variables across individuals. Final, SCN is a data-driven way, without any prior clinical hypothesis, to detect possible abnormal regions/connections/network patterns at the whole brain scale in TLE; future hypothesis-driven experiment is needed to verify the findings of our work.

5 | CONCLUSION

This study demonstrated T1w/T2w reductions in the frontotemporal and thalamic regions and extensive disconnections of an mSCN, providing evidence that TLE is a system disorder with widespread disruptions at regional and network levels. The T1w/T2w laterality of the

putamen at baseline was altered and negatively related with the hippocampus in TLE. Furthermore, ATL surgery increased T1w/T2w values in the ipsilateral putamen. This finding suggested that the putamen may play a transfer station role in damage spreading induced by epileptic seizures from the hippocampus. Last, we found identifiable differences of T1w/T2w changes between LTLE and RTLE, revealed by more increased connections and decreased global efficiency of a covariance network in LTLE.

AUTHOR CONTRIBUTIONS

Cheng Luo and Dongmei An designed the study and supervised the project. Yingjie Qin, Le Zhang, Xin Tong, Fenglai Xiao, Qiyong Gong, and Dong Zhou managed the experiments and data collection. Yuchao Jiang and Wei Li undertook the data analysis. Yuchao Jiang wrote the manuscript, which was revised by Wei Li, Sisi Jiang, Dongmei An, Yunfang Li, Dezhong Yao, and Cheng Luo. All authors reviewed the manuscript and approved the final manuscript.

ACKNOWLEDGEMENTS

This work was partly supported by the grants from the National Natural Science Foundation of China (No. grant number: U2033271, 61933003, 81960249, and 81901730); the CAMS Innovation Fund for Medical Sciences (CIFMS) (No. 2019-I2M-5-039); China Postdoctoral Science Foundation (Nos. BX2021078 and 2021M700852); Shanghai Sailing Program from Shanghai Science and Technology Committee (22YF1402800); the Natural Science Foundation of Sichuan (23NSFSC0016 and 22NSFSC0530); and the Sichuan Provincial Program of Traditional Chinese Medicine (2021ZD017). The authors gratefully acknowledge the participation of the study subjects and investigators.

CONFLICT OF INTEREST

The authors declare no conflict of interest.

DATA AVAILABILITY STATEMENT

The data (T1w/T2w data) supporting the findings of this study are available from the corresponding author upon reasonable request.

ORCID

Yuchao Jiang https://orcid.org/0000-0001-7012-0559
Sisi Jiang https://orcid.org/0000-0002-7430-9639
Qiyong Gong https://orcid.org/0000-0002-5912-4871
Dong Zhou https://orcid.org/0000-0001-7101-4125
Cheng Luo https://orcid.org/0000-0003-0524-5886

REFERENCES

Agcaoglu, O., Miller, R., Mayer, A. R., Hugdahl, K., & Calhoun, V. D. (2015). Lateralization of resting state networks and relationship to age and gender. *NeuroImage*, *104*, 310–325. https://doi.org/10.1016/j.neuroimage.2014.09.001

Alexander-Bloch, A., Giedd, J. N., & Bullmore, E. (2013). Imaging structural co-variance between human brain regions. *Nature Reviews. Neuroscience*, *14*(5), 322–336. https://doi.org/10.1038/nrn3465

Bernhardt, B. C., Bernasconi, N., Hong, S. J., Dery, S., & Bernasconi, A. (2016). Subregional mesiotemporal network topology is altered in temporal lobe epilepsy. *Cerebral Cortex*, *26*(7), 3237–3248. https://doi.org/10.1093/cercor/bhv166

Bernhardt, B. C., Bonilha, L., & Gross, D. W. (2015). Network analysis for a network disorder: The emerging role of graph theory in the study of epilepsy. *Epilepsy & Behavior*, *50*, 162–170. https://doi.org/10.1016/j.yebeh.2015.06.005

Bernhardt, B. C., Chen, Z., He, Y., Evans, A. C., & Bernasconi, N. (2011). Graph-theoretical analysis reveals disrupted small-world organization of cortical thickness correlation networks in temporal lobe epilepsy. *Cerebral Cortex*, *21*(9), 2147–2157. https://doi.org/10.1093/cercor/bhq291

Bernhardt, B. C., Hong, S., Bernasconi, A., & Bernasconi, N. (2013). Imaging structural and functional brain networks in temporal lobe epilepsy. *Frontiers in Human Neuroscience*, *7*, 624. https://doi.org/10.3389/fnhum.2013.00624

Besson, P., Dinkelacker, V., Valabregue, R., Thivard, L., Leclerc, X., Baulac, M., … Dupont, S. (2014). Structural connectivity differences in left and right temporal lobe epilepsy. *NeuroImage*, *100*, 135–144. https://doi.org/10.1016/j.neuroimage.2014.04.071

Bettus, G., Bartolomei, F., Confort-Gouny, S., Guedj, E., Chauvel, P., Cozzone, P. J., … Guye, M. (2010). Role of resting state functional connectivity MRI in presurgical investigation of mesial temporal lobe epilepsy. *Journal of Neurology, Neurosurgery, and Psychiatry*, *81*(10), 1147–1154. https://doi.org/10.1136/jnnp.2009.191460

Bland, B. H. (2004). The power of theta: Providing insights into the role of the hippocampal formation in sensorimotor integration. *Hippocampus*, *14*(5), 537–538. https://doi.org/10.1002/hipo.20027

Bonilha, L., Alessio, A., Rorden, C., Baylis, G., Damasceno, B. P., Min, L. L., & Cendes, F. (2007). Extrahippocampal gray matter atrophy and memory impairment in patients with medial temporal lobe epilepsy. *Human Brain Mapping*, *28*(12), 1376–1390. https://doi.org/10.1002/hbm.20373

Caciagli, L., Bernasconi, A., Wiebe, S., Koepp, M. J., Bernasconi, N., & Bernhardt, B. C. (2017). A meta-analysis on progressive atrophy in intractable temporal lobe epilepsy: Time is brain? *Neurology*, *89*(5), 506–516. https://doi.org/10.1212/WNL.0000000000004176

Chao, L. L., Tosun, D., Woodward, S. H., Kaufer, D., & Neylan, T. C. (2015). Preliminary evidence of increased hippocampal myelin content in veterans with posttraumatic stress disorder. *Frontiers in Behavioral Neuroscience*, *9*, 333. https://doi.org/10.3389/fnbeh.2015.00333

Chumbley, J. R., & Friston, K. J. (2009). False discovery rate revisited: FDR and topological inference using Gaussian random fields. *NeuroImage*, *44*(1), 62–70. https://doi.org/10.1016/j.neuroimage.2008.05.021

de Campos, B. M., Coan, A. C., Lin Yasuda, C., Casseb, R. F., & Cendes, F. (2016). Large-scale brain networks are distinctly affected in right and left mesial temporal lobe epilepsy. *Human Brain Mapping*, *37*(9), 3137–3152. https://doi.org/10.1002/hbm.23231

Desikan, R. S., Segonne, F., Fischl, B., Quinn, B. T., Dickerson, B. C., Blacker, D., … Killiany, R. J. (2006). An automated labeling system for subdividing the human cerebral cortex on MRI scans into gyral based regions of interest. *NeuroImage*, *31*(3), 968–980. https://doi.org/10.1016/j.neuroimage.2006.01.021

Dreifuss, S., Vingerhoets, F. J., Lazeyras, F., Andino, S. G., Spinelli, L., Delavelle, J., & Seeck, M. (2001). Volumetric measurements of subcortical nuclei in patients with temporal lobe epilepsy. *Neurology*, *57*(9), 1636–1641. https://doi.org/10.1212/wnl.57.9.1636

Drenthen, G. S., Backes, W. H., Aldenkamp, A. P., Vermeulen, R. J., Klinkenberg, S., & Jansen, J. F. A. (2020). On the merits of non-invasive myelin imaging in epilepsy, a literature review. *Journal of Neuroscience Methods*, *338*, 108687. https://doi.org/10.1016/j.jneumeth.2020.108687

Drenthen, G. S., Fonseca Wald, E. L. A., Backes, W. H., Debeij-Van Hall, M., Hendriksen, J. G. M., Aldenkamp, A. P., … Jansen, J. F. A. (2019). Lower myelin-water content of the frontal lobe in childhood absence epilepsy. *Epilepsia*, *60*(8), 1689–1696. https://doi.org/10.1111/epi.16280

Duan, M., Chen, X., He, H., Jiang, Y., Jiang, S., Xie, Q., … Yao, D. (2015). Altered basal ganglia network integration in schizophrenia. *Frontiers in Human Neuroscience*, *9*, 561. https://doi.org/10.3389/fnhum.2015.00561

Fisher, R. S., Cross, J. H., French, J. A., Higurashi, N., Hirsch, E., Jansen, F. E., … Zuberi, S. M. (2017). Operational classification of seizure types by the international league against Epilepsy: Position paper of the ILAE Commission for Classification and Terminology. *Epilepsia*, *58*(4), 522–530. https://doi.org/10.1111/epi.13670

Focke, N. K., Yogarajah, M., Bonelli, S. B., Bartlett, P. A., Symms, M. R., & Duncan, J. S. (2008). Voxel-based diffusion tensor imaging in patients with mesial temporal lobe epilepsy and hippocampal sclerosis. *NeuroImage*, *40*(2), 728–737. https://doi.org/10.1016/j.neuroimage.2007.12.031

Ganzetti, M., Wenderoth, N., & Mantini, D. (2014). Whole brain myelin mapping using T1- and T2-weighted MR imaging data. *Frontiers in Human Neuroscience*, *8*, 671. https://doi.org/10.3389/fnhum.2014.00671

Ganzetti, M., Wenderoth, N., & Mantini, D. (2015). Mapping pathological changes in brain structure by combining T1- and T2-weighted MR imaging data. *Neuroradiology*, *57*(9), 917–928. https://doi.org/10.1007/s00234-015-1550-4

Garbelli, R., Milesi, G., Medici, V., Villani, F., Didato, G., Deleo, F., … Spreafico, R. (2012). Blurring in patients with temporal lobe epilepsy: Clinical, high-field imaging and ultrastructural study. *Brain*, *135*(Pt 8), 2337–2349. https://doi.org/10.1093/brain/aws149

Glasser, M. F., & Van Essen, D. C. (2011). Mapping human cortical areas in vivo based on myelin content as revealed by T1- and T2-weighted MRI. *The Journal of Neuroscience*, *31*(32), 11597–11616. https://doi.org/10.1523/JNEUROSCI.2180-11.2011

Granberg, T., Fan, Q., Treaba, C. A., Ouellette, R., Herranz, E., Mangeat, G., … Mainero, C. (2017). In vivo characterization of cortical and white matter neuroaxonal pathology in early multiple sclerosis. *Brain*, *140*(11), 2912–2926. https://doi.org/10.1093/brain/awx247

Guye, M., Regis, J., Tamura, M., Wendling, F., McGonigal, A., Chauvel, P., & Bartolomei, F. (2006). The role of corticothalamic coupling in human temporal lobe epilepsy. *Brain*, *129*(Pt 7), 1917–1928. https://doi.org/10.1093/brain/awl151

Haneef, Z., Lenartowicz, A., Yeh, H. J., Levin, H. S., Engel, J., Jr., & Stern, J. M. (2014). Functional connectivity of hippocampal networks in temporal lobe epilepsy. *Epilepsia*, *55*(1), 137–145. https://doi.org/10.1111/epi.12476

Hwang, G., Dabbs, K., Conant, L., Nair, V. A., Mathis, J., Almane, D. N., … Hermann, B. (2019). Cognitive slowing and its underlying neurobiology in temporal lobe epilepsy. *Cortex*, *117*, 41–52. https://doi.org/10.1016/j.cortex.2019.02.022

Keller, S. S., Wieshmann, U. C., Mackay, C. E., Denby, C. E., Webb, J., & Roberts, N. (2002). Voxel based morphometry of grey matter abnormalities in patients with medically intractable temporal lobe epilepsy: Effects of side of seizure onset and epilepsy duration. *Journal of Neurology, Neurosurgery, and Psychiatry*, *73*(6), 648–655. https://doi.org/10.1136/jnnp.73.6.648

Kemmotsu, N., Girard, H. M., Bernhardt, B. C., Bonilha, L., Lin, J. J., Tecoma, E. S., … McDonald, C. R. (2011). MRI analysis in temporal lobe epilepsy: Cortical thinning and white matter disruptions are related to side of seizure onset. *Epilepsia*, *52*(12), 2257–2266. https://doi.org/10.1111/j.1528-1167.2011.03278.x

Kim, J. S., Koo, D. L., Joo, E. Y., Kim, S. T., Seo, D. W., & Hong, S. B. (2016). Asymmetric gray matter volume changes associated with epilepsy duration and seizure frequency in temporal-lobe-epilepsy patients with favorable surgical outcome. *Journal of Clinical Neurology*, *12*(3), 323–331. https://doi.org/10.3988/jcn.2016.12.3.323

Lariviere, S., Bernasconi, A., Bernasconi, N., & Bernhardt, B. C. (2021). Connectome biomarkers of drug-resistant epilepsy. *Epilepsia*, *62*(1), 6–24. https://doi.org/10.1111/epi.16753

Lariviere, S., Rodriguez-Cruces, R., Royer, J., Caligiuri, M. E., Epilepsy, E., Labate, A., … McDonald, C. (2021). Structural covariance network changes in the common epilepsies: A worldwide ENIGMA study. Paper presented at the Epilepsia.

Lei, D., Li, K., Li, L., Chen, F., Huang, X., Lui, S., … Gong, Q. (2015). Disrupted functional brain connectome in patients with posttraumatic stress disorder. *Radiology*, *276*(3), 818–827. https://doi.org/10.1148/radiol.15141700

Li, W., An, D., Tong, X., Liu, W., Xiao, F., Ren, J., … Zhou, D. (2019). Different patterns of white matter changes after successful surgery of mesial temporal lobe epilepsy. *NeuroImage: Clinical*, *21*, 101631. https://doi.org/10.1016/j.nicl.2018.101631

Li, W., Jiang, Y., Qin, Y., Zhou, B., Lei, D., Luo, C., … An, D. (2021). Dynamic gray matter and intrinsic activity changes after epilepsy surgery. *Acta Neurologica Scandinavica*, *143*(3), 261–270. https://doi.org/10.1111/ane.13361

Liu, M., Bernhardt, B. C., Bernasconi, A., & Bernasconi, N. (2016). Gray matter structural compromise is equally distributed in left and right temporal lobe epilepsy. *Human Brain Mapping*, *37*(2), 515–524. https://doi.org/10.1002/hbm.23046

Melie-Garcia, L., Slater, D., Ruef, A., Sanabria-Diaz, G., Preisig, M., Kherif, F., … Lutti, A. (2018). Networks of myelin covariance. *Human Brain Mapping*, *39*(4), 1532–1554. https://doi.org/10.1002/hbm.23929

Mori, S., Oishi, K., Jiang, H., Jiang, L., Li, X., Akhter, K., … Mazziotta, J. (2008). Stereotaxic white matter atlas based on diffusion tensor imaging in an ICBM template. *NeuroImage*, *40*(2), 570–582. https://doi.org/10.1016/j.neuroimage.2007.12.035

Palaniyappan, L., Park, B., Balain, V., Dangi, R., & Liddle, P. (2015). Abnormalities in structural covariance of cortical gyrification in schizophrenia. *Brain Structure & Function*, *220*(4), 2059–2071. https://doi.org/10.1007/s00429-014-0772-2

Pustina, D., Avants, B., Sperling, M., Gorniak, R., He, X., Doucet, G., … Tracy, J. (2015). Predicting the laterality of temporal lobe epilepsy from PET, MRI, and DTI: A multimodal study. *NeuroImage: Clinical*, *9*, 20–31. https://doi.org/10.1016/j.nicl.2015.07.010

Pustina, D., Doucet, G., Sperling, M., Sharan, A., & Tracy, J. (2015). Increased microstructural white matter correlations in left, but not right, temporal lobe epilepsy. *Human Brain Mapping*, *36*(1), 85–98. https://doi.org/10.1002/hbm.22614

Reyes, A., Kaestner, E., Bahrami, N., Balachandra, A., Hegde, M., Paul, B. M., … McDonald, C. R. (2019). Cognitive phenotypes in temporal lobe epilepsy are associated with distinct patterns of white matter network abnormalities. *Neurology*, *92*(17), e1957–e1968. https://doi.org/10.1212/WNL.0000000000007370

Royer, J., Bernhardt, B. C., Lariviere, S., Gleichgerrcht, E., Vorderwulbecke, B. J., Vulliemoz, S., & Bonilha, L. (2022). Epilepsy and brain network hubs. *Epilepsia*, *63*(3), 537–550. https://doi.org/10.1111/epi.17171

Rubinov, M., & Sporns, O. (2010). Complex network measures of brain connectivity: Uses and interpretations. *NeuroImage*, *52*(3), 1059–1069. https://doi.org/10.1016/j.neuroimage.2009.10.003

Shah, P., Bassett, D. S., Wisse, L. E. M., Detre, J. A., Stein, J. M., Yushkevich, P. A., … Davis, K. A. (2019). Structural and functional asymmetry of medial temporal subregions in unilateral temporal lobe epilepsy: A 7T MRI study. *Human Brain Mapping*, *40*(8), 2390–2398. https://doi.org/10.1002/hbm.24530

Thom, M., Holton, J. L., D'Arrigo, C., Griffin, B., Beckett, A., Sisodiya, S., … Sander, J. W. (2000). Microdysgenesis with abnormal cortical myelinated fibres in temporal lobe epilepsy: A histopathological study with calbindin D-28-K immunohistochemistry. *Neuropathology and Applied Neurobiology*, *26*(3), 251–257.

Vandewouw, M. M., Young, J. M., Shroff, M. M., Taylor, M. J., & Sled, J. G. (2019). Altered myelin maturation in four year old children born very

preterm. *NeuroImage: Clinical*, *21*, 101635. https://doi.org/10.1016/j.nicl.2018.101635

Wang, K. L., Hu, W., Liu, T. H., Zhao, X. B., Han, C. L., Xia, X. T., … Meng, F. G. (2019). Metabolic covariance networks combining graph theory measuring aberrant topological patterns in mesial temporal lobe epilepsy. *CNS Neuroscience & Therapeutics*, *25*(3), 396–408. https://doi.org/10.1111/cns.13073

Wiebe, S., & Jette, N. (2012). Pharmacoresistance and the role of surgery in difficult to treat epilepsy. *Nature Reviews. Neurology*, *8*(12), 669–677. https://doi.org/10.1038/nrneurol.2012.181

Winston, G. P., Stretton, J., Sidhu, M. K., Symms, M. R., & Duncan, J. S. (2014). Progressive white matter changes following anterior temporal lobe resection for epilepsy. *NeuroImage: Clinical*, *4*, 190–200. https://doi.org/10.1016/j.nicl.2013.12.004

Zuo, X. N., Kelly, C., Di Martino, A., Mennes, M., Margulies, D. S., Bangaru, S., … Milham, M. P. (2010). Growing together and growing apart: Regional and sex differences in the lifespan developmental trajectories of functional homotopy. *The Journal of Neuroscience*, *30*(45), 15034–15043. https://doi.org/10.1523/JNEUROSCI.2612-10.2010

SUPPORTING INFORMATION

Additional supporting information can be found online in the Supporting Information section at the end of this article.

How to cite this article: Jiang, Y., Li, W., Qin, Y., Zhang, L., Tong, X., Xiao, F., Jiang, S., Li, Y., Gong, Q., Zhou, D., An, D., Yao, D., & Luo, C. (2023). In vivo characterization of magnetic resonance imaging-based T1w/T2w ratios reveals myelin-related changes in temporal lobe epilepsy. *Human Brain Mapping*, *44*(6), 2323–2335. https://doi.org/10.1002/hbm.26212